Journal of Neurocytology **31**, 41–48 (2002)

Different Ca^{2+} dynamics between isolated hippocampal pyramidal cells and dentate granule cells

ATSUSHI BABA, MAKI K. YAMADA, NOBUYOSHI NISHIYAMA, NORIO MATSUKI and YUJI IKEGAYA*

Laboratory of Chemical Pharmacology, Graduate School of Pharmaceutical Sciences, The University of Tokyo, Tokyo 113-0033, Japan
ikegaya@tk.airnet.ne.jp

Received 22 July 2002; revised 1 Novermber 2002; accepted 5 Novermber 2002

Abstract

The hippocampal formation contains a variety of neuronal types. The principal neurons are granule cells in the dentate gyrus and pyramidal cells in Ammon's horn. These two neuron types show distinct cell morphology and display a different vulnerability to ischemic injury or various neurotoxins. In order to illustrate the difference in the pathophysiological properties of these neurons, we established a method for separately culturing granule cells and pyramidal cells. They were prepared from the dentate gyrus and Ammon's horn of 3-day-old Wistar rat pups and maintained for 7–9 days in culture. After transient exposure to *N*-methyl-D-aspartate or glutamate, both the cultured neuron populations displayed somatic Ca^{2+} transients with similar amplitudes, but the subsequent recovery to baseline was about twice as fast in granule cells than in pyramidal cells. Similar results were obtained for K^+ depolarization-induced Ca^{2+} elevation, suggesting that the relatively rapid Ca^{2+} clearance in granule cells is independent of Ca^{2+} influx pathways. The present study provides the first evidence for a difference in Ca^{2+} dynamics and homeostasis between granule and pyramidal cells and may represent a cellular basis for the differential vulnerability of hippocampal neurons.

Introduction

The hippocampus is one of the most vulnerable brain regions regarding neuronal cell loss and injury. In some neuropathologic conditions, including Alzheimer's disease, epilepsy, cerebral ischemia, anadrenalism and exposure to excitatory amino acids or certain types of bioactive agents (*e.g.*, colchicine, potassium cyanide), neurodegeneration occurs consistently both *in vivo* and *in vitro*, but susceptible cell populations vary according to the nature of the damaging insults. Indeed, two principal neuron types of the hippocampal formation, *i.e.*, granule cells of the dentate gyrus and pyramidal cells of Ammon's horn, display a distinct pattern of vulnerability to the insults. In Alzheimer's disease, epilepsy and ischemia, primarily pyramidal neurons undergo degeneration (Kirino, 1982; Probst *et al.*, 1983; Sloviter, 1983) and display a high vulnerability to excitatory amino acids, *e.g.*, glutamate and *N*-methyl-D-aspartate (NMDA), termed excitotoxicity (Mattson & Kater, 1989; Choi & Rothman, 1990; Vornov *et al.*, 1991; Ikegaya *et al.*, 2001). On the other hand, granule cells undergo selective damage following exposure to cytoskeleton-disrupting agents, *e.g.*, colchicine and cytochalasin (Kim *et al.*, 2002).

Loss of hippocampal pyramidal cells after ischemic and excitotoxic injuries often results from perturbation of Ca^{2+} homeostasis. Experimental evidence shows that abnormally sustained elevation of intracellular Ca^{2+} concentrations ($[Ca^{2+}]_i$) causes irreversible neurodegeneration probably through aberrant recruitment of Ca^{2+}-activated enzymes such as proteases and phospholipases (Tontchev & Yamashima, 1999). Conversely, cytoskeleton disruption-induced death of granule cells is virtually independent of Ca^{2+} entry (Kim *et al.*, 2002). Interestingly, our recent study has shown that the characteristic susceptibility of pyramidal and granule cells is retained after removal of their afferents and efferents in organotypic slice cultures (Ikegaya & Matsuki, 2002), suggesting that the selective vulnerability does not depend on neural circuits but rather is attributable to intrinsic cell

*To whom correspondence should be addressed.

0300–4864

properties. We therefore hypothesize that intracellular Ca^{2+} behaves differently in granule and pyramidal cells, thereby resulting in their differing vulnerability to neurotoxins.

To address the possible heterogeneity in Ca^{2+} homeostasis, these two neuron types were prepared from the dentate gyrus and Ammon's horn of rat pups, and separately maintained for 7–9 days in culture. Here we report that the neurons display different Ca^{2+} dynamics; granule cells show a more rapid decay of excitotoxin-evoked $[Ca^{2+}]_i$ increases. Our findings may account for the intrinsic mechanisms underlying the neuron type-specific vulnerability.

Materials and methods

ASTROCYTE-CONDITIONED MEDIUM

Astrocyte-conditioned medium was obtained from primary cultures of cortical astrocytes. Glial cell cultures were prepared from postnatal 2-day-old Wistar/ST rat pups (SLC, Shizuoka, Japan) and maintained in Eagle's minimum essential medium (Nissui Pharmaceuticals, Tokyo, Japan) supplemented with 30 mM glucose, 2 mM L-glutamine, 1 mM pyruvate and 10% fetal bovine serum (Cell Culture Technologies, Cleveland, OH, USA), as described previously (Suzuki *et al.*, 2001). In brief, cortical hemispheres were dissected out and pooled into Leibovitz's L-15 medium. After removing meninges, cells were dissociated by 0.25% trypsinization (Difco, Detroit, MI, USA) and 0.01% deoxyribonuclease I (DNase I) (Sigma, St. Louis, MO, USA) at 37°C for 40 min. The cell suspension was then centrifuged at 250 *g* for 5 min, and the pellet was mechanically dissociated by being passed 5–12 times through a plastic tip with an 850-μm hole. After filtration through double nylon nets (45-μm mesh) to remove cell clumps, cells were placed into 75-cm^2 culture flasks (Falcon, Oxnard, CA, USA) at a density of 1×10^6 cells/cm^2. Cultures were maintained in a humidified, 5% CO_2 incubator at 37°C. The medium was changed every 3–4 days. After the cultures became confluent, the fresh medium was conditioned for 3 days, filtrated through a 0.22-μm-pore membrane, and then used for neuron culture as astrocyte-conditioned medium.

PRIMARY CULTURES OF GRANULE AND PYRAMIDAL CELLS

Neurons were cultivated in Neurobasal (Life Technologies, Gaithersburg, MD, USA) supplemented with 0.5 mM L-glutamine and 2% B-27 (Life Technologies). Three-day-old Wistar/ST rats (SLC) were deeply anesthetized by ether, and the hippocampal formation was immediately dissected out and placed in ice-cold Gey's balanced salt solution bubbled with a gas mixture of 95% O_2 and 5% CO_2. After removal of the subicular complex along the sulcus hippocampi, the remaining part was divided into the dentate gyrus and Ammon's horn with extreme care so that cultures contained neurons predominantly from these parts of the hippocampal formation (Fig. 1). Both tissues were cut into pieces and treated with 0.25% trypsin (Difco) and 0.01% DNase I (Sigma)

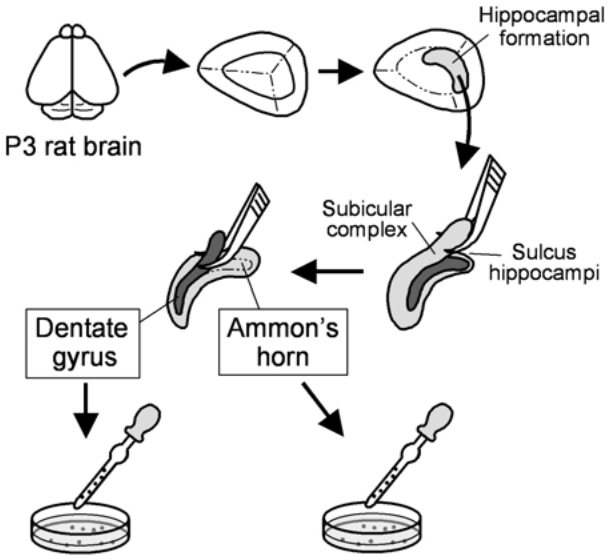

Fig. 1. Experimental procedures for preparing cultures of two distinct neuron types from the dentate gyrus and Ammon's horn of the hippocampal formation. The hippocampal formation was dissected out from the brain of a 3-day-old Wistar rat. After removing the subicular complex, the dentate gyrus and Ammon's horn were carefully separated across the length along the sulcus hippocampi prior to trypsinization.

at 37°C for 30 min. The incubation was terminated by addition of heat-inactivated horse serum (Cell Culture Technologies). The tissue fragments were centrifuged at 250 *g* for 5 min, the supernatant was removed, and the pellet was re-suspended in a mixture of 50% Neurobasal/B-27 and 50% astrocyte-conditioned medium. The suspension was gently triturated by being passed 3–5 times through a plastic tip with an 850-μm hole until visibly dispersed, followed by filtration through double nylon nets (45-μm mesh). We could obtain from each region about 2.0×10^5 cells per brain. The cells were plated at a density of 5.0×10^4 cells/cm^2 onto poly-L-lysine-coated 48-well cell culture plates (Costar, Cambridge, MA, USA). For immunohistochemical experiments or calcium imaging, cells were plated onto 15-mm glass microcoverslips (Matsunami, Osaka, Japan) coated with 0.1% polyethylenimine (Sigma). They were cultivated at 37°C in a humidified 5% CO_2 and 95% air atmosphere. To prevent proliferation of glial cells, the culture medium was changed to the conditioned medium-free Neurobasal/B-27 medium supplemented with 2 μM cytosine-D-arabino-furanoside (Sigma) 24 hr after the plating. Half of the medium was exchanged every 3 days.

NISSL STAINING

At day 7 *in vitro*, cultures were washed three times with 0.1 M phosphate-buffered saline (PBS) for 5 min at room temperature and fixed with 4% paraformaldehyde at 4°C for 30 min. After being washed with PBS for 3×15 min, they were incubated with 0.1% cresyl violet (Sigma) for 5 min at room temperature, followed by a 5-min wash with PBS. The average diameters of the cell body of granule

and pyramidal cells were measured using a micrometer microscope.

IMMUNOFLUORESCENCE IMAGING

Cultured granule and pyramidal cells were immunolabeled with mouse monoclonal antibody against calbindin D_{28k} (Sigma) and rabbit polyclonal antibody against microtubule-associated protein-2 (MAP-2) (Chemicon, Temecula, CA, USA). At day 7 *in vitro*, they were fixed with 4% paraformaldehyde in PBS at 4°C for 30 min. The cells were then washed three times with PBS, permeabilized with 0.1% Triton X-100 in PBS for 15 min at room temperature, and then washed three times with PBS again. Nonspecific antibody binding was blocked by incubation with 2% goat serum (Vector Laboratories, Burlingame, CA, USA) in PBS for 60 min at room temperature. Without wash, the cultures were incubated with primary antibodies against calbindin D_{28k} (1:200) and MAP-2 (1:1000) overnight at 4°C. They were washed three times with PBS for 30 min and incubated with Alexa 488- or Alexa 594-conjugated secondary antibodies (each 1:1000, Molecular Probes, Eugene, OR, USA) diluted in 2% goat serum-containing PBS for 60 min at room temperature. The immunofluorescent preparations were then washed three times with PBS. Fluorescent images were obtained with an MRC-1000 confocal imaging system (Bio-Rad Microscience Division, Cambridge, MA, USA).

Ca^{2+} IMAGING

Changes in $[Ca^{2+}]_i$ in cell bodies were detected by a standard microfluorometrical technique using fura-2, as previously described (Shitaka *et al.*, 1996). Briefly, cells plated onto coverslips were incubated in Neurobasal medium (Life Technologies) containing 10 μM fura-2 acetoxymethyl ester (Wako Chemicals, Osaka, Japan) and 0.02% cremophor EL (Sigma) at 37°C for 60 min. They were then rinsed with HEPES-buffered balanced salt solution consisting of (in mM) 130 NaCl, 5 KCl, 1.8 $CaCl_2$, 10 D-glucose, 20 HEPES and 0.001 tetrodotoxin, adjusted to pH 7.4 with NaOH. The coverslip with the fura-2-loaded cells was placed in a laminar flow perfusion chamber and constantly perfused with the same solution at 37°C at a rate of 3 ml/min. The perfusion chamber was mounted on the stage of an inverted microscope (Nikon, Tokyo, Japan). Pre-selected fields were illuminated by a xenon light source through a Nikon 20× objective. The image analysis system AQUACOSMOS (Hamamatsu Photonics, Hamamatsu, Japan) was used to monitor the ratio of the intensity of fura-2 fluorescence excited at 340 nm and 360 nm. Emitted fluorescence was imaged with a charge-coupled device camera (Orca ERII, Hamamatsu Photonics). In all experiments, the signal at each wavelength with the shutter closed was obtained for background subtraction. For calibration of $[Ca^{2+}]_i$, 10 μM fura-2 was suspended in standard 50 mM PIPES-KOH buffer (pH 6.8), containing EGTA and $CaCl_2$ at calculated ratios (Harafuji & Ogawa, 1980) and illuminated by 340 nm and 360 nm beams alternately, and the fluorescence was monitored at 510 nm *in vitro* (Kudo & Ogura, 1986). Glutamate (Wako) or NMDA (Sigma) was applied from a local perfusion pipette consisting of an array of 280 μm inner diameter capillary tubes positioned within 200 μm from the cells (around 300 μl/min). To test voltage-dependent Ca^{2+} responses, the cells were depolarized with 50 mM K^+ solution (KCl was substituted for equimolar NaCl in the perfusate), which was applied for 10 sec through the same pipette. Baseline responses were obtained for 5 min prior to the addition of agonists or high K^+ solution. The decay of $[Ca^{2+}]_i$ transients could be well fitted with a mono-exponential function of time (t): $F(t) = A \times e^{-t/\tau}$, where A and τ are amplitude and time constant, respectively. In all sets of experiments, the experimental data were collected from more than three independent trials.

STATISTICS

Data were subjected to Student's t-test in Table 1. Unless otherwise specified, data are expressed as means ± S.E.M. Significance was defined at the $P < 0.05$ level.

Table 1. Summary of $[Ca^{2+}]_i$ dynamics after various types of stimulation. Neurons were exposed for 10 sec to 10 μM NMDA, 10 or 100 μM glutamate, or high-K^+ solution. Amplitude indicates the peak $[Ca^{2+}]_i$.

		Dentate gyrus		*Ammon's horn*	
Treatment		*N*	*Mean ± S.E.M.*	*N*	*Mean ± S.E.M.*
Amplitude (nM)					
NMDA	10 μM	35	76.4 ± 6.4	36	66.1 ± 6.1
Glutamate	10 μM	22	72.5 ± 9.5	21	64.3 ± 6.4
Glutamate	100 μM	29	102.5 ± 6.0	24	109.4 ± 12.6
High K^+	50 mM	51	79.3 ± 6.8	56	72.8 ± 6.4
Decay constant (sec)					
NMDA	10 μM	35	41.8 ± 2.8	36	79.3 ± 5.4*
Glutamate	10 μM	22	24.1 ± 2.2	21	43.7 ± 11.1**
Glutamate	100 μM	29	35.1 ± 2.8	24	73.1 ± 13.1**
High K^+	50 mM	51	71.2 ± 5.1	56	104.9 ± 9.7**

Data are means ± S.E.M. of N cases, obtained from 3–7 independent experiments, each of which contains 5–10 neurons.
* $P < 0.01$; ** $P < 0.05$ vs. dentate gyrus: Student's t-test.

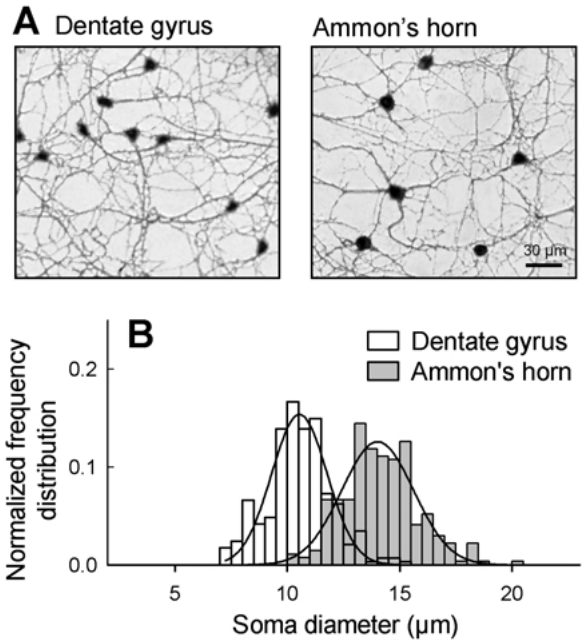

Fig. 2. Soma-size difference between cultured dentate gyrus and Ammon's horn cells. (A) Nissl images of cells prepared from the dentate gyrus (left) and Ammon's horn (right). Cultures were stained with cresyl violet at day 7 *in vitro*. (B) Distribution of the soma diameters of 288 and 277 cells prepared from the dentate gyrus (white columns) and Ammon's horn (gray columns), respectively. The ordinate indicates normalized frequency. Each trace represents an approximate unimodal Gaussian distribution with a mean $\pm$ S.D. of 10.54 ± 1.23 μm for the dentate gyrus or 14.02 ± 1.60 μm for the Ammon's horn.

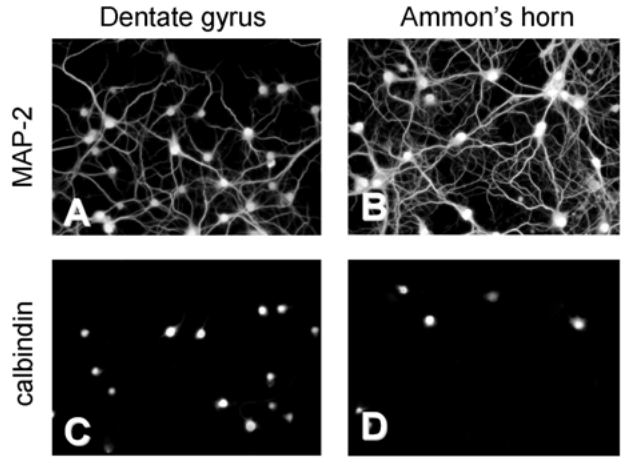

Fig. 3. Immunoreactivity for calbindin D_{28k} in dentate gyrus neurons and Ammon's neurons. Neurons prepared from the dentate gyrus (A,C) and Ammon's horn (B,D) were immunolabeled with anti-MAP-2 antibody (A,B) and anti-calbindin D_{28k} antibody (C,D) at day 7 *in vitro*.

Results

TWO DISTINCT NEURON CULTURES PREPARED FROM THE HIPPOCAMPAL FORMATION

Cells were prepared from two different hippocampal subregions, *i.e.*, the dentate gyrus and Ammon's horn, of neonatal rats (Fig. 1). At day 7 in culture, the majority of cells prepared from both subregions developed neurites and connected with one another to form a fairly dense mesh-like networks (Fig. 2A). Thus, they were morphologically identifiable as neurons, as previously reported (Boss *et al.*, 1987; Mattson & Kater, 1989). To ensure the validity of our cell-isolation method, we focused on the soma sizes of these cultured cells, based on previous studies showing that the soma size of a granule cell is smaller than that of a pyramidal cell *in vivo* (Amaral & Witter, 1995). We measured the diameters of the somata of all cells with neuron-like morphology in 10 randomly selected microscopic fields. The soma sizes exhibited two discrete unimodal Gaussian distributions; the average size was 10.5 ± 1.2 μm for dentate gyrus cultures and 14.0 ± 1.6 μm for Ammon's horn cultures (means $\pm$ S.D. of 288 and 277 cells, respectively, $P < 0.01$, Student's *t*-test) (Fig. 2B), indicating that we had succeeded in separating two different populations of neurons from the hippocampal formation.

As further confirmation, the cultures were processed for immunolabelling with anti-calbindin D_{28k} and anti-MAP-2 antibodies. Calbindin D_{28k} is a member of the EF-hand family of Ca^{2+}-binding proteins (Baimbridge *et al.*, 1992) and mainly expressed in dentate granule cells and Ammon's horn interneurons *in vivo*. (Jande *et al.*, 1981; Baimbridge and Miller, 1982; Seress *et al.*, 1993). Therefore, we expected that our dentate gyrus cultures would contain more numerous calbindin-immunopositive neurons than Ammon's horn cultures. As shown in the representative confocal images of Figure 3, the dentate gyrus neurons actually showed more evident immunoreactivity for calbindin D_{28k}; the ratios of calbindin-positive to MAP-2-positive neurons were $46.0 \pm 2.0\%$ for dentate gyrus cultures and $12.3 \pm 1.1\%$ for Ammon's horn cultures (means $\pm$ S.D. of each 3 independent experiments, $P < 0.01$, Student's *t*-test). Not all dentate gyrus neurons were calbindin-positive under our culture conditions. This is probably because they were relatively recently formed cells. Indeed, about 40% of rat granule cells develop around postnatal day 3 (Schlessinger *et al.*, 1975), and it is not until full maturation that newly formed granule cells exhibit abundant expression of calbindin D_{28k} (Cameron *et al.*, 1993). Our result is, therefore, consistent with an *in vivo* study showing that only 30–40% of granule cells were immunopositive for calbindin D_{28k} in rats at 3 days of age (Rami *et al.*, 1987). We therefore concluded that our cultures of dentate gyrus neurons and Ammon's horn neurons predominantly contained granule cells and pyramidal cells, respectively.

HETEROGENEITY IN INTRACELLULAR Ca^{2+} MOBILITY

The role of neuronal calbindin D_{28k} is still unknown, but one hypothesis proposes that the protein binds Ca^{2+} with high affinity and thereby regulates Ca^{2+} signaling dynamics and neuronal excitability (Baimbridge *et al.*, 1992; Lledo *et al.*, 1992; Chard *et al.*, 1993; Airaksinen *et al.*, 1997). We therefore addressed the assumed difference in Ca^{2+} dynamics between calbindin-rich granule cells and calbindin-poor pyramidal cells. The cells were loaded with the Ca^{2+} indicator fura-2, and $[Ca^{2+}]_i$ was determined by its fluorescence ratio in the soma, in which calbindin D_{28k} was strongly expressed (Fig. 3C,D). The fluorescence intensity of fura-2 excited at 360 nm in wavelength (F_{360} value) did not differ between the two types of neuron: 613.6 ± 33.1 in granule cells and 673.8 ± 33.1 in pyramidal cells (arbitrary unit, means $\pm$ S.E.M. of 90 and 89, respectively, $P > 0.1$, Student's *t*-test), nor did the resting levels of $[Ca^{2+}]_i$, which were calculated from the ratio $F_{340/360}$: 54.8 ± 1.7 nM in granule cells ($N = 110$) and 60.1 ± 2.4 nM in pyramidal cells ($N = 109$, $P > 0.1$). Therefore, the efficiency of fura-2 loading and the resting Ca^{2+} levels were equivalent between cultured granule and pyramidal cells.

When the glutamate receptor agonist NMDA was applied at a concentration of 10 μM for 10 sec, both granule and pyramidal cells showed a rapid increase in $[Ca^{2+}]_i$ and a subsequent recovery to baseline (Fig. 4).

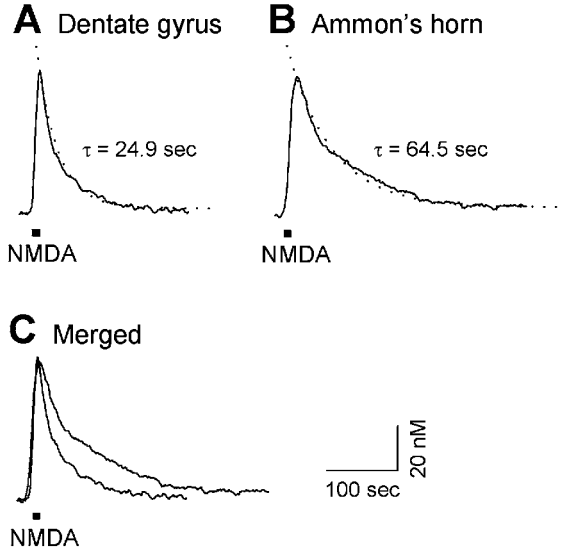

Fig. 4. Rapid decay of Ca^{2+} transients in dentate gyrus neurons. Cultured neurons were loaded with 10 μM fura2/AM at day 7–9 *in vitro* to monitor somatic $[Ca^{2+}]_i$ dynamics. Representative traces of $[Ca^{2+}]_i$ transients induced by 10-sec exposure to 10 μM NMDA were obtained from each one neuron of the dentate gyrus (A) and Ammon's horn (B). They were analyzed with ordinary least-squares regression techniques to determine the decay constants (τ) of mono-exponential functions. Both are superimposed in (C).

Interestingly, the peak amplitude of the $[Ca^{2+}]_i$ transient was not significantly different between these two types of neuron but the decay kinetics were substantially more rapid in granule cells (Fig. 4); the mean decay constant in granule cells was about half of that in pyramidal cells (Table 1). The results of other stimulants are summarized in Table 1. In both neuron types, exposure to glutamate for 10 sec caused similar $[Ca^{2+}]_i$ transients in a concentration-dependent manner but the return to baseline was always more rapid in granule cells (Table 1). Our preliminary experiments showed that the inhibition of NMDA responses by 10 μM ifenprodil, an inhibitor of NR2B-containing NMDA receptors, did not seem to differ between granule cells and pyramidal cells ($n = 9$, unpublished data), suggesting that the difference in Ca^{2+} dynamics were not ascribable to differential NMDA receptor subtypes.

To examine whether or not the different decay kinetics depend on Ca^{2+} influx pathways, we evaluated the $[Ca^{2+}]_i$ elevation induced by brief depolarization (50 mM K^+ for 10 sec). High K^+-evoked $[Ca^{2+}]_i$ transients were efficiently blocked by 10 μM nicardipine, a L-type Ca^{2+} channel blocker ($82.2 \pm 4.9\%$ and $89.4 \pm 4.1\%$ decreases in amplitude, means $\pm$ S.E.M. of 14 granule cells and 17 pyramidal cells, respectively, both $P < 0.01$) but not by 100 μM AP5, a NMDA receptor antagonist ($14.6 \pm 10.2\%$ and $8.6 \pm 8.3\%$ decreases in 15 granule cells and 13 pyramidal cells, respectively, both $P < 0.1$). Thus, K^+ depolarization induced NMDA receptor-independent Ca^2 influx, nonetheless, granule cells still displayed $[Ca^{2+}]_i$ transients with a more rapid decay than pyramidal cells in response to high K^+ (Table 1).

Discussion

Tightly regulated $[Ca^{2+}]_i$ fluctuations have been proposed to be cellular events that determine neuronal vulnerability during development and diseases as well as regulate neuronal functions, including synaptic plasticity, rhythmic activity generation, and spatiotemporal summation of neural information. Elucidating the cellular processes controlling Ca^{2+} homeostasis is, therefore, an important step to understand the multiplicity in information processing and neuronal vulnerability among various neurons. Although Lee *et al.* (2000) have reported differential Ca^{2+}-buffering properties between excitatory and inhibitory hippocampal neurons, little is known about a diversity in $[Ca^{2+}]_i$ dynamics amongst principal excitatory neurons in the hippocampal formation, *i.e.*, granule cells and pyramidal cells, in spite of the fact that they show a remarkable difference in vulnerability to pathological or chemical insults. In the present study, we have established a technique for isolating and culturing granule and pyramidal cells separately and have shown for the

first time that these neurons display distinct kinetics of $[Ca^{2+}]_i$ changes in response to glutamate receptor activation and depolarization, providing a possible explanation for the heterogeneity of neuronal physiology and pathology.

Although both granule and pyramidal cells extended MAP-2-positive neurites and developed finely woven networks in culture, the histogram of the soma sizes displayed two discrete Gaussian distributions, and immunoreactivity for calbindin D_{28k} was more evident in granule cell cultures as compared with pyramidal cell cultures. Therefore, our experimental procedure proved effective for separation of granule and pyramidal cells. Our recent study has already utilized a part of this isolation method in order to investigate neuronal vulnerability, also confirming that the separated neurons were selectively susceptible to colchicine or NMDA (Ikegaya & Matsuki, 2002). Hence, this culture system is amenable for direct study of variations in neuronal properties in this region of the brain.

By monitoring changes in the fluorescence intensity of fura-2, we found that granule cells had faster clearing speeds of somatic $[Ca^{2+}]_i$ transients than pyramidal cells. Because of the high Ca^{2+} affinity of this indicator, care must be taken in carrying out and interpreting the data analysis (Stout & Reynolds, 1999); lopsided incorporation or overloading of fura-2 would lead to an unexpected alteration in $[Ca^{2+}]_i$ decay kinetics by the Ca^{2+}-buffering ability of fura-2 itself. In our experiments, however, this is not the case. First, the F_{360} values did not differ between granule and pyramidal cells. This indicates that comparable amounts of fura-2 were loaded into these neurons. Second, higher concentrations of glutamate produced $[Ca^{2+}]_i$ transients with larger amplitudes. This suggests that the fura-2 fluorescence was not saturated at least in 10 μM glutamate-induced $[Ca^{2+}]_i$ transients. Under these reliable conditions, the $[Ca^{2+}]_i$ decay kinetics in granule cells was readily proven to be faster than that in pyramidal cells, indicating more efficient Ca^{2+} clearance in granule cells. Interestingly, the efficient clearance was independent of Ca^{2+} influx pathway; the difference between granule and pyramidal cells was always observed across various stimuli, *i.e.*, NMDA, glutamate and K^+ depolarization. Thus, we consider that the differences in $[Ca^{2+}]_i$ kinetics were attributable to intrinsic variation in the Ca^{2+}-buffering or Ca^{2+}-extrusion ability of granule and pyramidal cells.

This raises the question of what intrinsic factor is involved in the rapid $[Ca^{2+}]_i$ decay in granule cells? Although most mammalian cells possess similar cytoplasmic and plasma membrane mechanisms for Ca^{2+} sequestration, their contribution differs significantly among cell types (Berridge *et al.*, 2000). Cellular models of Ca^{2+} diffusion have demonstrated that Ca^{2+} signal depend on the affinity and concentration of endogenous Ca^{2+} buffer (Roberts, 1994; Naraghi & Neher, 1997). Calbindin D_{28k} has been identified as such a potent Ca^{2+}-bindng protein. For example, Ca^{2+} signaling is severely suppressed by the intracellular application of calbindin D_{28k} protein (Chard *et al.*, 1993) or by transfection with calbindin D_{28k} gene (Lledo *et al.*, 1992) and enhanced by null mutation of the calbindin D_{28k} gene (Airaksinen *et al.*, 1997). The observation of abundant expression of the calbindin D_{28k} in granule cells might, therefore, be compatible with their higher ability of Ca^{2+} clearance. We do not believe, however, that the presence of calbindin D_{28k} in granule cells offers a sole explanation for the rapid Ca^{2+} clearance. In our cultures, only half of granule cells were immunonegative for calbindin D_{28k}, but we found no evidence for a corresponding variety in the $[Ca^{2+}]_i$ decay kinetics of granule cells (data not shown).

Another possibility may be provided by a difference in Ca^{2+} excretion mechanisms. Cytoplasmic Ca^{2+} is promptly removed by smooth endoplasmic reticulum calcium ATPases (SERCA) pumps and by plasma membrane Na^+-Ca^{2+} exchangers or Ca^{2+}-ATPases. In our cultured neurons, the contribution of the SERCA pumps is almost negligible because preliminary experiments revealed that the SERCA pump inhibitor thapsigargin (1 μM) minimally affected $[Ca^{2+}]_i$ decay kinetics in either granule or pyramidal cells (unpublished data). Thus, the Ca^{2+} clearance is mainly mediated by plasma membrane Na^+-Ca^{2+} exchangers or Ca^{2+}-ATPases. Assuming that these Ca^{2+}-extrusion machineries are evenly distributed over the plasma membrane, clearance apparently scales linearly with the surface, rather than the volume, of the soma. In this case, it is plausible that a smaller neuron, *i.e.*, a granule cell, displayed a higher ability of Ca^{2+} clearance than a pyramidal cell because of different 'surface to volume' ratios. We therefore consider that several intricate factors, including calbindin and cell surface area, are involved in the diversity of Ca^{2+} dynamics.

In the present study, we have established a cell type-specific differences in $[Ca^{2+}]_i$ dynamics in cultured hippocampal neurons. Weak Ca^{2+} buffering in a pyramidal cell may partly account for its vulnerability to Ca^{2+}-relevant injuries, *e.g.*, ischemia, seizure and excitotoxins. In addition, intracellular Ca^{2+} is known to serve as a regulator of many neuronal events, including synaptic vesicle docking (Cousin, 2000), synaptic plasticity (Bliss & Collingridge, 1993), filopodia motility (Acebes & Ferrús, 2000) and nuclear gene transcription (Santella & Carafoli, 1997). Further investigation of the heterogeneity in $[Ca^{2+}]_i$ dynamics would lead to new insights into the diversity of physiological and pathological properties of neurons.

Acknowledgments

This work was supported in part by Grant-in-Aid for Science Research from the Ministry of Education,

Culture, Sports, Science and Technology of Japan and by the Research Grant for Longevity Science (13-2) from the Ministry of Health, Labor and Welfare of Japan.

References

ACEBES, A. & FERRÚS, A. (2000) Cellular and molecular features of axon collaterals and dendrites. *Trends in Neurosciences* **23**, 557–565.

AIRAKSINEN, M. S., EILERS, J., GARASCHUK, O., THOENEN, H., KONNERTH, A. & MEYER, M. (1997) Ataxia and altered dendritic calcium signaling in mice carrying a targeted null mutation of the calbindin D28k gene. *Proceedings of the National Academy of Sciences of the USA* **94**, 1488–1493.

AMARAL, D. G. & WITTER, M. P. (1995) Hippocampal formation. In: *The Rat Nervous System*, edited by Paxinos, G. San Diego: Academic Press, pp. 443–492.

BAIMBRIDGE, K. G., CELIO, M. R. & ROGERS, J. H. (1992) Calcium-binding proteins in the nervous system. *Trends in Neurosciences* **15**, 303–308.

BAIMBRIDGE, K. G. & MILLER, J. J. (1982) Immunohistochemical localization of calcium-binding protein in the cerebellum, hippocampal formation and olfactory bulb of the rat. *Brain Research* **245**, 223–229.

BERRIDGE, M. J., LIPP, P. & BOOTMAN, M. D. (2000) The versatility and universality of calcium signalling. *Nature Reviews Molecular Cell Biology* **1**, 11–21.

BLISS, T. V. & COLLINGRIDGE, G. L. (1993) A synaptic model of memory: Long-term potentiation in the hippocampus. *Nature* **361**, 31–39.

BOSS, B. D., GOZES, I. & COWAN, W. M. (1987) The survival of dentate gyrus neurons in dissociated culture. *Brain Research* **433**, 199–218.

CAMERON, H. A., WOOLLEY, C. S., MCEWEN, B. S. & GOULD, E. (1993) Differentiation of newly born neurons and glia in the dentate gyrus of the adult rat. *Neuroscience* **56**, 337–344.

CHARD, P. S., BLEAKMAN, D., CHRISTAKOS, S., FULLMER, C. S. & MILLER, R. J. (1993) Calcium buffering properties of calbindin D_{28k} and parvalbumin in rat sensory neurones. *Journal of Physiology* **472**, 341–357.

CHOI, D. W. & ROTHMAN, S. M. (1990) The role of glutamate neurotoxicity in hypoxic-ischemic neuronal death. *Annual Review of Neuroscience* **13**, 171–182.

COUSIN, M. A. (2000) Synaptic vesicle endocytosis: Calcium works overtime in the nerve terminal. *Molecular Neurobiology* **22**, 115–128.

HARAFUJI, H. & OGAWA, Y. (1980) Re-examination of the apparent binding constant of ethylene glycol bis(β-aminoethyl ether)-N,N,N′,N′-tetraacetic acid with calcium around neutral pH. *Journal of Biochemistry* **87**, 1305–1312.

IKEGAYA, Y., KIM, J. A., BABA, M., IWATSUBO, T., NISHIYAMA, N. & MATSUKI, N. (2001) Rapid and reversible changes in dendrite morphology and synaptic efficacy following NMDA receptor activation: Implication for a cellular defense against excitotoxicity. *Journal of Cell Science* **114**, 4083–4093.

IKEGAYA, Y. & MATSUKI, N. (2002) Regionally selective neurotoxicity of NMDA and colchicine is independent of hippocampal neural circuitry. *Neuroscience* **113**, 253–256.

JANDE, S. S., MALER, L. & LAWSON, D. E. (1981) Immunohistochemical mapping of vitamin D-dependent calcium-binding protein in brain. *Nature* **294**, 765–767.

KIM, J.-A., MITSUKAWA, K., YAMADA, M. K., NISHIYAMA, N., MATSUKI, N. & IKEGAYA, Y. (2002) Cytoskeleton disruption causes apoptotic degeneration of dentate granule cells in hippocampal slice cultures. *Neuropharmacology* **42**, 1109–1118.

KIRINO, T. (1982) Delayed neuronal death in the gerbil hippocampus following ischemia. *Brain Research* **239,** 57–69.

KUDO, Y. & OGURA, A. (1986) Glutamate-induced increase in intracellular Ca^{2+} concentration in isolated hippocampal neurones. *British Journal of Pharmacology* **89**, 191–198.

LEE, S.-H., ROSENMUND, C., SCHWALLER, B. & NEHER, E. (2000) Differences in Ca^{2+} buffering properties between excitatory and inhibitory hippocampal neurons from the rat. *Journal of Physiology (London)* **525**, 405–418.

LLEDO, P. M., SOMASUNDARAM, B., MORTON, A. J., EMSON, P. C. & MASON, W. T. (1992) Stable transfection of calbindin-D_{28k} into the GH3 cell line alters calcium currents and intracellular calcium homeostasis. *Neuron* **9**, 943–954.

MATTSON, M. P. & KATER, S. B. (1989) Development and selective neurodegeneration in cell cultures from different hippocampal regions. *Brain Research* **490**, 110–125.

NARAGHI, M. & NEHER, E. (1997) Linearized buffered Ca^{2+} diffusion in microdomains and its implications for calculation of $[Ca^{2+}]$ at the month of a calcium channel. *Journal of Neuroscience* **17**, 6961–6973.

PROBST, A., BASLER, V., BRON, B. & ULRICH, J. (1983) Neuritic plaques in senile dementia of Alzheimer type: A Golgi analysis in the hippocampal region. *Brain Research* **268**, 249–254.

RAMI, A., BREHIER, A., THOMASSET, M. & RABIE, A. (1987) Cholecalcin (28-kDa calcium-binding protein) in the rat hippocampus: Development in normal animals and in altered thyroid states. An immunocytochemical study. *Developmental Biology* **124**, 228–238.

ROBERTS, W. M. (1994) Localization of calcium signals by a mobile calcium buffer in frog saccular hair cells. *Journal of Neuroscience* **14**, 3246–3262.

SANTELLA, L. & CARAFOLI, E. (1997) Calcium signaling in the cell nucleus. *FASEB Journal* **11**, 1091–1109.

SCHLESSINGER, A. R., COWAN, W. M. & GOTTLIEB, D. I. (1975) An autoradiographic study of the time of origin and the pattern of granule cell migration in the dentate gyrus of the rat. *Journal of Comparative Neurology* **159**, 149–175.

SERESS, L., GULYAS, A. I., FERRER, I., TUNON, T., SORIANO, E. & FREUND, T. F. (1993) Distribution, morphological features, and synaptic connections of parvalbumin- and calbindin D_{28k}-immunoreactive neurons in the human hippocampal formation. *Journal of Comparative Neurology* **337**, 208–230.

SHITAKA, Y., MATSUKI, N., SAITO, H. & KATSUKI, H. (1996) Basic fibroblast growth factor increases functional L-type Ca^{2+} channels in fetal rat hippocampal neurons: Implications for neurite morphogenesis *in vitro*. *Journal of Neuroscience* **16**, 6476–6489.

SLOVITER, R. S. (1983) "Epileptic" brain damage in rats induced by sustained electrical stimulation of the perforant path. I. Acute electrophysiological and light microscopic studies. *Brain Research Bulletin* **10**, 675–697.

STOUT, A. K. & REYNOLDS, I. J. (1999) High-affinity calcium indicators underestimate increases in intracellular calcium concentrations associated with excitotoxic glutamate stimulations. *Neuroscience* **89**, 91–100.

SUZUKI, K., IKEGAYA, Y., MATSUURA, S., KANAI, Y., ENDOU, H. & MATSUKI, N. (2001) Transient upregulation of the glial glutamate transporter GLAST in response to fibroblast growth factor, insulin-like growth factor and epidermal growth factor in cultured astrocytes. *Journal of Cell Science* **114**, 3717–3725.

TONTCHEV, A. B. & YAMASHIMA, T. (1999) Ischemic delayed neuronal death: Role of the cysteine proteases calpain and cathepsins. *Neuropathology* **19**, 356–365.

VORNOV, J. J., TASKER, R. C. & COYLE, J. T. (1991) Direct observation of the agonist-specific regional vulnerability to glutamate, NMDA, and kainate neurotoxicity in organotypic hippocampal cultures. *Experimental Neurology* **114**, 11–22.